

AD-757 342

Integrated Optical Circuits

**Naval Electronics
Laboratory Center**

**prepared for
Advanced Research Projects Agency**

JANUARY 1973

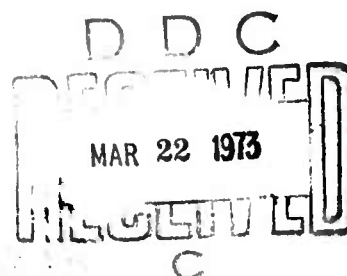
Distributed By:



**National Technical Information Service
U. S. DEPARTMENT OF COMMERCE**

AD757342

INTEGRATED OPTICAL CIRCUITS



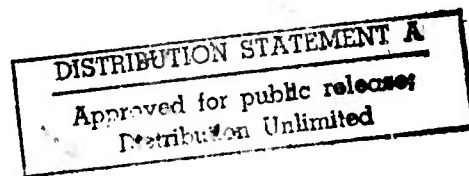
Demonstrates optical waveguiding and electrooptic modulation in diffused-layer and heteroepitaxial thin-film semiconductor structures; theoretically analyzes optical propagation in fiber-optic waveguides.

D. B. Hall

Research and Development

30 January 1973

Reproduced by
NATIONAL TECHNICAL
INFORMATION SERVICE
U.S. Department of Commerce
Springfield VA 22151



NAVAL ELECTRONICS LABORATORY CENTER
SAN DIEGO, CALIFORNIA 92152

27 R

UNCLASSIFIED

Security Classification

DOCUMENT CONTROL DATA - R & D

(Security classification of title, body of abstract and indexing annotation must be entered when the overall report is classified)

1. ORIGINATING ACTIVITY (Corporate author)	2a. REPORT SECURITY CLASSIFICATION UNCLASSIFIED
Naval Electronics Laboratory Center San Diego, California 92152	2b. GROUP

3. REPORT TITLE

INTEGRATED OPTICAL CIRCUITS

4. DESCRIPTIVE NOTES (Type of report and inclusive dates)

Research and Development, 1 April 1972 to 1 October 1972

5. AUTHOR(S) (First name, middle initial, last name)

D. B. Hall

6. REPORT DATE 30 January 1973	7a. TOTAL NO. OF PAGES 2627	7b. NO. OF REFS 10
-----------------------------------	--------------------------------	-----------------------

8a. CONTRACT OR GRANT NO.

b. PROJECT NO. ARPA Order 2158, Amendment 1;
Program Code 3010; Contract
c. F215.01 (NELC Problem F215)

9a. ORIGINATOR'S REPORT NUMBER(S)

NELC TR 1861

9b. OTHER REPORT NO(S) (Any other numbers that may be assigned
this report)

10. DISTRIBUTION STATEMENT

Approved for public release; distribution unlimited

11. SUPPLEMENTARY NOTES

12. SPONSORING MILITARY ACTIVITY

Advanced Research Projects Agency

13. ABSTRACT

Partial work is reported on establishing the feasibility of integrated optics for use in high-capacity (multi-GHz) telecommunications and for implementing a militarily applicable, fiber-optic-transmission-line, multiterminal multiplexing system through low-loss coupling and modulation. More specifically, optical waveguiding in diffused-layer and heteroepitaxial thin-film semiconductor structures, both planar and three-dimensional, is demonstrated, as is electrooptic modulation in diffused-layer and heteroepitaxial thin-film semiconductor structures of high resistivity. In addition, optical propagation in fiber-optic waveguides is theoretically analyzed, and future areas of research and development (particularly pattern delineation and optical coupling) and theoretical analysis are outlined.

UNCLASSIFIED

Security Classification

14 KEY WORDS	LINK A		LINK B		LINK C	
	ROLE	WT	ROLE	WT	ROLE	WT
Diffused waveguide layers						
Electrooptic modulation						
Fiber optics						
Heteroepitaxial thin films						
Optical waveguiding						

PROBLEM

Advance the material and device physics of integrated optics for military applications; establish in concert with other Navy and DoD programs a continuing assessment of system requirements; produce prototype optical elements and subsystems which are aimed at satisfying these requirements. More specifically, establish the feasibility of integrated optics (1) for use in high-capacity (multi-GHz) telecommunications and (2) for implementing a militarily applicable, fiber-optic-transmission-line, multiterminal multiplexing system through low-loss coupling and modulation.

RESULTS

1. Optical waveguiding in diffused-layer and heteroepitaxial thin-film semiconductor structures, both planar and three dimensional, is demonstrated.
2. Electrooptic modulation is also demonstrated in diffused-layer and heteroepitaxial thin-film semiconductor structures of high resistivity.
3. Optical propagation in fiber-optic waveguides is theoretically analyzed.

RECOMMENDATIONS

1. Research the areas of (a) pattern delineation of miniature three-dimensional waveguides and related optical elements by photo- and electron-resist masking techniques and by ion beam milling, and (b) optical coupling of light into and out of integrated optic circuits, in particular using fiber-optic waveguides.
2. Continue theoretical analysis of optical propagation in a variety of waveguide structures to support the findings of this report and those of recommendation 1.

ADMINISTRATIVE INFORMATION

The work reported here was sponsored by the Advanced Research Projects Agency, Material Sciences, Arlington, Virginia, under ARPA Order 2158, Amendment 1; Program Code 3010; Contract F215.01 (NELC Problem F215). Work was performed from 1 April 1972 to 1 October 1972. Principal investigator was D. J. Albares of the NELC Electro-Optics Technology Division (Code 2500); associate investigators were D. B. Hall, W. E. Martin, and H. F. Taylor of Code 2500 and C. Yeh of the University of California, Los Angeles. This report was authored by D. B. Hall and approved for publication 30 January 1973.

CONTENTS

INTRODUCTION . . .	page 3
DIFFUSED WAVEGUIDES . . .	4
The Diffusion Process . . .	4
The Index Profile . . .	7
Waveguide Propagation . . .	8
HETEROEPITAXIAL WAVEGUIDES . . .	11
Leaky Modes . . .	11
Double-Layer Structures . . .	13
Electrooptic Phase Modulators . . .	13
FIBER-OPTICAL WAVEGUIDES . . .	16
Guided Waves in Inhomogeneous Fibers . . .	16
Dispersion of Pulses Passing Through Fibers or IOCs . . .	19
Noncircular Optical Guide . . .	20
SUMMARY AND PROJECTION . . .	21
REFERENCES . . .	24

TABLES

1	Selected Diffusions in ZnSe and CdS . . .	page 5
2	X-ray Analysis of Cadmium-Diffused ZnSe Powder . . .	8
3	Some Properties of II-VI and III-V Semiconductor Compounds . . .	11

ILLUSTRATIONS

1	Refractive index as a function of wavelength for the II-VIs . . .	page 5
2	Ideal refractive index profile for diffused waveguide . . .	7
3	Cutoff in waveguides with abrupt and linear index profiles . . .	9
4	Scattered light in a cadmium-diffused ZnSe channel guide of 2-by-12 μ m cross section . . .	10
5	Scattering losses in a 2-by-12 μ m channel guide . . .	10
6	Mode profiles of leaky waves from ZnSe heteroepitaxial layers . . .	12
7	Three double-layer heteroepitaxial structures . . .	13
8	ZnSe heteroepitaxial thin-film phase modulator . . .	15
9	Intensity modulator setup . . .	15

INTRODUCTION

The fabrication of miniature solid-state optical components, both active and passive, and thin-film waveguides to link them on semiconductor or dielectric substrates is becoming possible with the advancement of such disciplines as the material sciences, quantum electronics, and optics. Integrated optical components — such as sources, detectors, modulators, and various coupling elements — on one or more tiny substrates will comprise systems much smaller in size and weight than conventional optical devices. The new systems will be much less susceptible to environmental hazards such as mechanical vibrations, extremes in temperature, and electromagnetic fluctuations; their small size will make it easy to isolate and shield them from such effects. In addition, active components such as wideband electro-optic modulators can be operated at very low voltage and power levels because of the small dimensions involved.

In particular, thin-film optical components have found an important potential use in the area of high-bandwidth optical communications because of the recent rapid progress in the fabrication of extremely low-loss fiber-optic waveguides. Fiber-optic waveguides with losses as low as 4dB/km at the $0.85\mu\text{m}$ GaAs and $1.06\mu\text{m}$ Nd-YAG laser wavelengths, and also single-mode fibers with bandwidths as high as 10GHz for a 1km length, immensely widen the horizon in optical communications. However, techniques must be found to process efficiently the optical information transmitted by the fibers at bit rates approaching the bandwidth capacity of the fibers.

Integrated optics could perform a number of functions in the area of high-bandwidth optical communications. They include rapid modulation and switching by thin-film elements using applied electric fields to generate small electrooptic index changes, coupling, filtering of signals, detection by p-n or other junction structures in thin films, and optical generation and amplification by thin-film laser elements.

For military applications, fiber-optic systems also offer important benefits, such as freedom from electromagnetic interference, elimination of grounding problems, and security (no signal leakage), as well as the potential for enormous size, weight, and cost savings. In addition to high-capacity point-to-point communications, a major interest in integrated optics from a military standpoint is the potential for implementing a fiber-optic-transmission-line, multiterminal multiplexing system through low-loss coupling and modulation elements. This would provide isolated-terminal, redundant, information transfer, thus facilitating the truly modular (including distributed computer) command control and communication system.

The objective of the program reported here is to advance the material and device physics of integrated optics for military applications, to establish in concert with other Navy and DoD programs a continuing assessment of system requirements, and to produce prototype optical elements and subsystems that are aimed at satisfying these requirements.

The task of circuit conception and design will be a continuing one, stemming from the technology and application assessment. Through the

program. elementary circuits and subsystems will be fabricated, and an experimental IOC fiber-optic communication system will be investigated.

Presently, work is beginning on establishing the feasibility of integrated optics for performing some of the functions listed above. At NELC in the past six months, a variety of passive-waveguide and electrooptic-waveguide modulator structures have been fabricated, tested, and evaluated. Optical guiding and electrooptic phase modulation have been demonstrated at 6328A in: (1) mixed single-crystal layers formed by the solid-state diffusion of cadmium or selenium into single-crystal substrates of ZnSe, CdS, and ZnS, and (2) heteroepitaxial layers of ZnS and ZnSe deposited on GaAs substrates.

In particular, the cadmium-diffused ZnSe structures and the ZnSe-on-GaAs heteroepitaxial films are promising candidates for optical waveguides and waveguide modulators in integrated optical circuits operating in the visible or near infrared. Planar and three-dimensional channel guides have been made in these structures with losses of less than 3dB/cm and with efficient electrooptic intensity modulation in lengths of the order of 0.5cm.

In addition to the work done at NELC, theoretical work at the University of California, Los Angeles, has proceeded on the propagation characteristics of guided light along glass fibers (see FIBER-OPTICAL WAVEGUIDES, below). In particular, computer programs have been developed to solve in a reasonably straightforward way the difficult problem of guided-wave propagation in fibers with an arbitrary radial index profile. This is useful for obtaining solutions in inhomogeneous fibers such as Selfoc.

DIFFUSED WAVEGUIDES

THE DIFFUSION PROCESS

Increases of up to 5% in the refractive index can be effected in II-VI single-crystal films by the substitutional solid-state diffusion of cadmium or selenium into the host crystal. The layers thus formed are single crystal with an optical quality in some cases approaching that of the substrate. Figure 1 is a plot of refractive index as a function of wavelength for the II-VIs. Both ZnSe and CdS have higher indices than ZnS; therefore, the replacement of either zinc by cadmium or sulfur by selenium in ZnS will raise the index. Similar arguments apply to the replacement of zinc by cadmium to raise the index of ZnSe and the replacement of sulfur by selenium to raise the index of CdS. All these diffusions have been performed successfully. Tellurium diffusions into ZnSe to replace the selenium with tellurium in order to raise the index have also been tried; however, they have been unsuccessful, yielding surface layers with extreme surface damage which do not guide light.

The diffusions are produced by sealed ampoule techniques. The appropriate amounts of diffusants and the polished single-crystal substrate to be diffused are placed within a cleaned quartz ampoule and sealed prior to baking. The details of the procedure have been published, and table 1

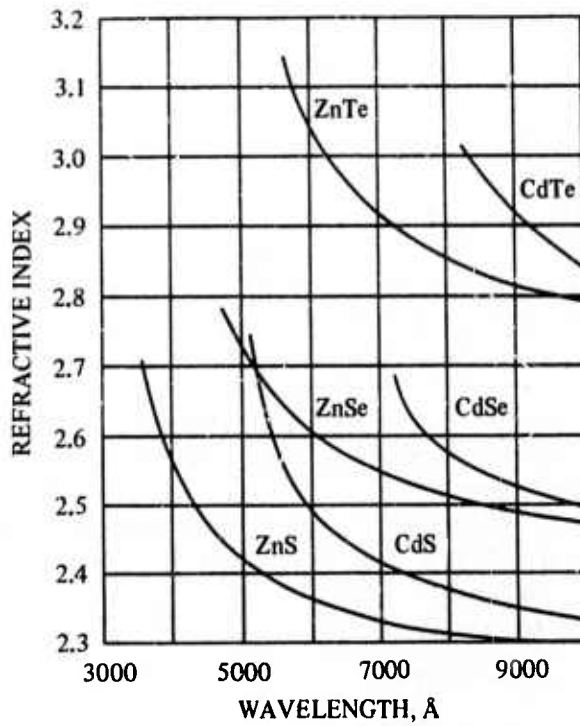


Figure 1. Refractive index as a function of wavelength for the II-VIs.

gives representative numbers for two selected diffusions in ZnSe and CdS (ref. 1 and 2).

TABLE I. SELECTED DIFFUSIONS IN ZnSe AND CdS.

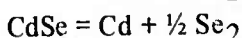
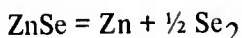
Substrate	ZnSe	CdS
Diffusant	Cd	Se
Temperature, °C	850	700
Ideal Gas or Saturation Pressure, atm	$P_{Cd} = 2.0$	$P_{Se_2} = 0.66$ $P_{Se_2} = 0.05$
Depth, μm	3	$3\frac{1}{2}$
Surface Composition	$Zn_{0.92}Cd_{0.08}Se$	$CdS_{0.95}Se_{0.05}$
Change in Refractive Index	0.02	0.02
Shift in Bandgap, Å	250	200

Two important problems that must be dealt with in making diffused optical waveguides which will have losses approaching the 1dB/cm loss figure considered desirable in integrated optics immediately come to mind. They are the obtaining of sufficiently large, high-optical-quality, II-VI single-crystal substrates and the minimizing of surface etching of the II-VI crystal substrate in the quartz ampoule during the diffusion

process, which produces surface roughness and consequential optical scattering losses.

The first problem is dependent on the state of the art in growing II-VI single-crystal substrates; one way around it would be to perform diffusions in the heteroepitaxial II-VI structures that are discussed below under HETEROEPITAXIAL WAVEGUIDES. Modifications in the diffusion process in the past month have largely solved the surface etching problem. In particular, excellent results have been obtained for cadmium-diffused ZnSe, where the crystal surface before and after diffusion looked completely smooth under microscope examination at 600X. More detailed examinations involving an electron beam scan of the surfaces for roughness will be done at the Hughes Research Laboratories with their SEM microprobe.

The quartz ampoule during the cadmium diffusions contains ZnSe powder, CdSe powder, and the ZnSe single-crystal substrate to be diffused. At the diffusion temperature of 850°C, the vapor species Zn, Cd, and Se₂ are in equilibrium with the ZnSe and CdSe powders and the ZnSe single crystal. We have the reactions



with dissociation constants

$$K_{\text{ZnSe}} = \frac{P_{\text{Zn}} [P_{\text{Se}_2}]^{\frac{1}{2}}}{[\text{ZnSe}]}$$

$$K_{\text{CdSe}} = \frac{P_{\text{Cd}} [P_{\text{Se}_2}]^{\frac{1}{2}}}{[\text{CdSe}]}$$

By choosing an equilibrium surface composition of Zn_{1-x}Cd_xSe, we obtain

$$\frac{x}{1-x} = \frac{[\text{CdSe}]}{[\text{ZnSe}]} = \frac{P_{\text{Cd}} K_{\text{ZnSe}}}{P_{\text{Zn}} K_{\text{CdSe}}}$$

where x can vary from 0 to 100%. The composition x is simply obtained by weighing out the CdSe and ZnSe powders in the correct mole fraction ratio x/(1-x).

Originally, cadmium metal instead of CdSe powder was placed in the ampoule for cadmium diffusion into ZnSe. For reasons still not well understood, predictable results were very difficult to obtain. In light of the improved results with CdSe powder, the II-VI compound powders CdS and CdSe, instead of the elemental powders selenium and sulfur, will be tried with selenium diffusions into CdS single crystals, and compound powders instead of elemental powders will be tried with cadmium and selenium diffusion into ZnS single crystals. Anticipated with these

changes are improvements in the quality of the diffused layers and ease in choosing the correct amounts of diffusants for generating suitable concentration gradients in the diffused layers.

THE INDEX PROFILE

In an ideal diffusion, the crystal is in an environment of a limitless amount of diffusant. The concentration gradient of diffusant within the crystal then follows a complementary error function curve falling from a maximum at the surface to a limiting value of zero deep enough within the substrate. Assuming the change in refractive index is proportional to the amount of diffusant, the index gradient also follows a complementary error function curve. Such an ideal index profile with representative numbers used in a typical diffusion is shown in figure 2.

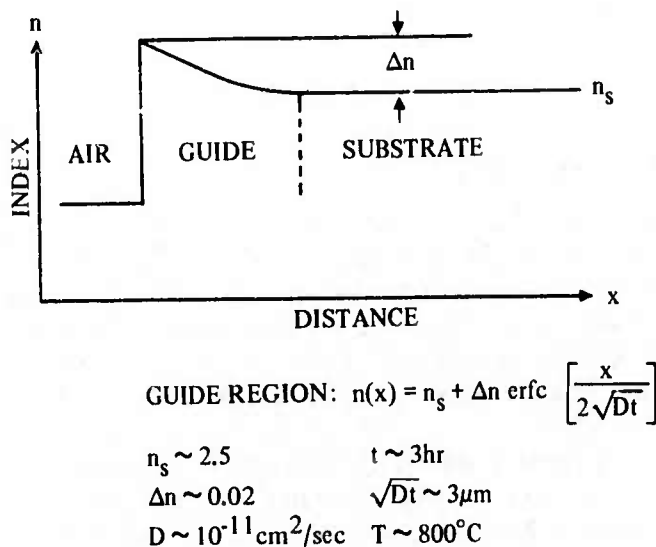


Figure 2. Ideal refractive index profile for diffused waveguide.

Index profiles have been determined in a number of the diffused waveguides by taking photoluminescence spectra at 77°K. Multiple measurements of the spectral position of a characteristic luminescence peak (for example, A exciton emission in $\text{CdS}_x\text{Se}_{1-x}$ or $\text{Zn}_{1-x}\text{Cd}_x\text{Se}$) between successive etches yield a plot of bandgap or crystal composition and, hence, index as a function of depth into the diffused layer. Most of the profiles do not fit a complementary error function curve, and more work must be done to understand them.

X-ray analyses on powdered portions of diffused material have also been made to determine the difference between the lattice constants of the diffused waveguide surface and the undiffused substrate interior, yielding the maximum changes in concentration and index between the two regions.

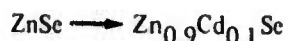
Some X-ray data are shown in table 2 which agree with photoluminescence measurements on the same sample.

Both techniques discussed above will probably be superseded by the potentially much more versatile technique of electron microprobe analysis.

TABLE 2. X-RAY ANALYSIS OF CADMIUM-DIFFUSED ZnSe POWDER.

$\lambda = 2d_{hkl} \sin \theta$			
hkl	d (Before), Å	d' (After), Å	(d' - d)/d, %
311	1.708	1.720	0.7
422	1.157	1.166	0.8
531	0.958	0.966	0.8

Lattice Constant Increase $\sim \frac{1}{3}$ of 1%



WAVEGUIDE PROPAGATION

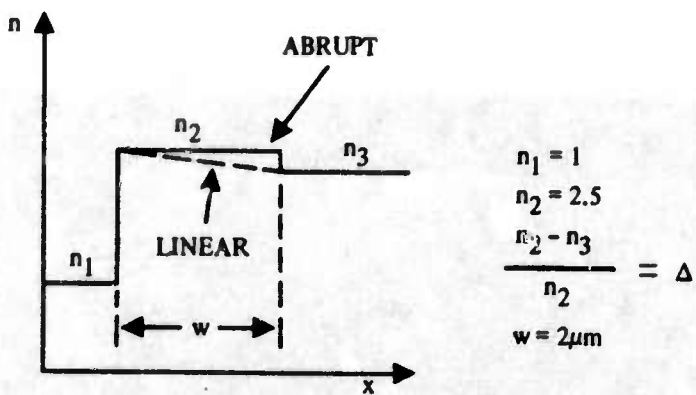
Planar diffused waveguides in which guiding has so far been observed have ranged in thickness between 2 and 12 μm (ref. 3). Waveguiding in them was studied by focusing the beam from a HeNe laser onto the cleaved end of the crystal with a microscope objective. The near-field output from the opposite end was viewed with the aid of a second microscope objective. The minimum thickness for guides that can be easily excited this way is about 2 μm .

For the purpose of evaluating optical propagation in these guides, the approximation of a linearly graded index model, as shown in figure 3, is used. The table included in figure 3 gives the threshold values of index difference for propagation of the lowest four TE modes for $\lambda = 0.633\mu\text{m}$ and a guide width of 2 μm . We see that there is single-mode propagation of just the TE_0 mode for an index difference between 0.16 and 1.1%.

A 1% change in index corresponding to single-mode propagation in guides less than about 2 μm thick and to propagation of just two modes in guides between about 2 and 3 $\frac{1}{2}\mu\text{m}$ thick is easy to attain in the diffused structures. For example, a 1% index difference corresponds to the change from a 0% mole fraction of cadmium to a 10% mole fraction in $\text{Zn}_{1-x}\text{Cd}_x\text{Se}$.

In addition to planar guides, three-dimensional channel guides have been fabricated in cadmium-diffused ZnSe and selenium-diffused CdS. Glass fibers were used as a shadow mask during an SiO evaporation on the substrate crystal. The subsequent diffusion step allowed penetration of the diffusant into the substrate only where the glass fibers had been. Channel guides with cross-sectional areas as small as 2 by 5 μm were made this way.

Optical losses were determined in the channel waveguides by measuring the attenuation of scattered power along the guide with a fiber-optic probe. In several of the $\text{Zn}_{1-x}\text{Cd}_x\text{Se}$ channel guides, losses less than 3dB/cm (limit of resolution for 5mm sample length) were recorded. Figure 4



MODE	Δ (ABRUPT), %	Δ (LINEAR), %
TE ₀	0.05	0.16
TE ₁	0.46	1.1
TE ₂	1.3	3.1
TE ₃	2.5	5.8

Figure 3. Cutoff in waveguides with abrupt and linear index profiles.

is a photograph of scattered light in a 2-by-1 $2\mu\text{m}$ $\text{Zn}_{1-x}\text{Cd}_x\text{Se}$ guide 4mm long and figure 5 depicts on a semilog plot scattered power as a function of position in that guide.

The polarization of the output light from the channel waveguides was also measured. In most of them, a considerable amount of mode conversion occurred; light entering these guides with TE linear polarization would exit with a large component of TM polarization. However, in the smallest guides, with 2-by-5 μm cross sections, no mode conversion occurred. This indicated that differences between the propagation velocities of the various modes were large enough so that coupling between them due to scattering centers in the guide or surface roughness was negligible. Much more work, especially theoretical, must be done to understand in detail these phenomena.



Figure 4. Scattered light in a cadmium-diffused ZnSe channel guide of 2-by-12 μ m cross section.

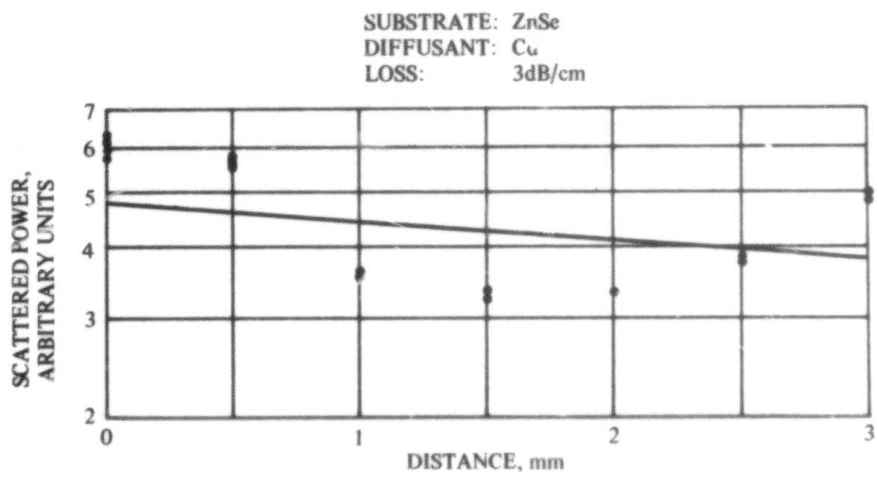


Figure 5. Scattering losses in a 2-by-12 μ m channel guide.

HETEROEPITAXIAL WAVEGUIDES

LEAKY MODES

Optical propagation has been observed in cubic heteroepitaxial films of ZnS on GaAs substrates purchased from the ITEK Corporation, Lexington, Massachusetts, and in cubic heteroepitaxial films of ZnSe and $ZnSe_{0.98}Te_{0.02}$ purchased from the Photo-electronic Materials Corporation, Washington, D.C. (ref. 4). The films ranged in thickness from 2 to 20 μm and in length up to nearly 1 inch. Losses as low as 3 dB/ μm were measured in the thicker films (9 or more μm thick) and much higher losses were observed in the thinner films.

Some of the material properties of ZnS, ZnSe, and GaAs along with the related compounds GaP, InAs, and ZnTe are listed in table 3. We see that there is less than a $\frac{1}{2}$ of 1% lattice mismatch between ZnSe and GaAs, indicating very little strain in the heteroepitaxial ZnSe layers on GaAs, and that there is a 4% mismatch for ZnS on GaAs, indicating more strain than in the ZnSe case.

TABLE 3. SOME PROPERTIES OF II-VI AND III-V SEMICONDUCTOR COMPOUNDS.

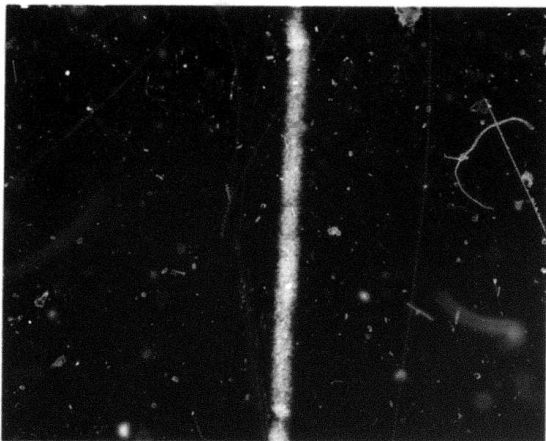
	Lattice Constant, \AA	Refractive Index at 1.96 eV*	Bandgap, eV	Electrooptic Coefficient $n^3 r_4 / (10^{-9} \text{ cm/V})$
ZnS	5.41	2.35	3.8	1.9
GaP	5.45	3.3	2.2	3.6
ZnSe	5.67	2.58	2.8	3.5
GaAs	5.65	3.9	1.4	4.3
ZnTe	6.09	2.98	2.4	8.6
InAs	6.05	3.9	0.35	

*1.96 eV = 6328 \AA

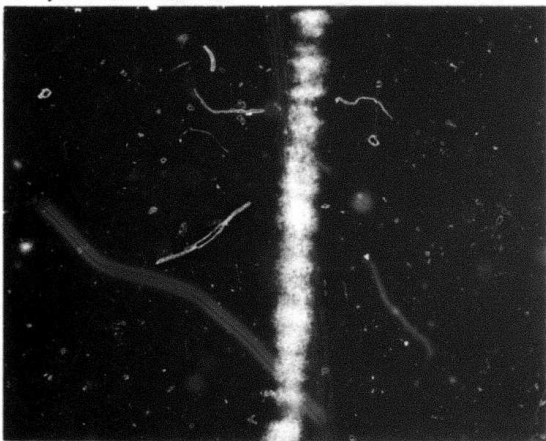
The refractive indices of the ZnS and ZnSe films are less than that of the GaAs substrate, so the heteroepitaxial films do not act as ordinary waveguides with total internal reflection of the guided light at the guide-substrate interface. However, optical propagation of the so-called leaky modes does occur, with attenuation losses inversely proportional to the cube of the film thickness and proportional to the square of the wavelength. At 6328 \AA , the attenuation rate due to light leakage into the substrate is of the order of 0.1 dB/cm in 15 μm thick films and 10 dB/cm in 4 μm thick films. Also, the loss rate for the TM polarization is several times higher than that for the TE polarization. Photographs of TE and TM near-field outputs from three different heteroepitaxial films of ZnSe are shown in figure 6. The films are:

A. ZnSe layer 2 μm thick, 2.2 mm long

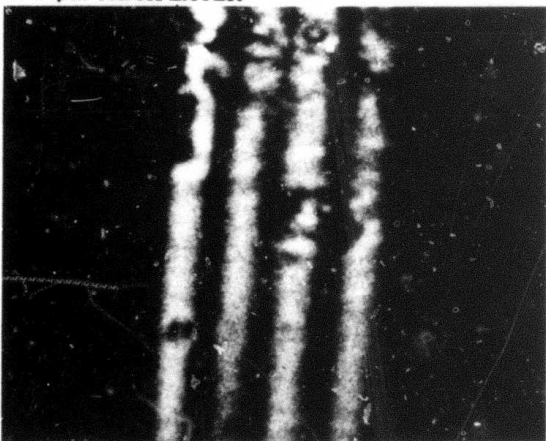
A. $2\mu\text{m}$ THICK LAYER



B. $4\mu\text{m}$ THICK LAYER TE_0



C. $14\mu\text{m}$ THICK LAYER TE_0



TM_0



TM_0

Figure 6. Mode profiles of leaky waves from ZnSe heteroepitaxial layers.

- B. ZnSe layer 4 μm thick, 8.6mm long
- C. ZnSe layer 14 μm thick, 11.5mm long

Layer A propagated just the TE_0 mode; layer B propagated the TE_0 and, with much higher losses, the TM_0 mode; and, in layer C, TE and TM modes up to the sixth order were observed.

DOUBLE-LAYER STRUCTURES

For the thinner heteroepitaxial films, the leaky modes are too lossy. Modified waveguide structures must be devised to avoid these losses. Figure 7 shows three suggested heteroepitaxial structures in which guiding occurs in the top layer with no leakage losses because of the low-index second layer between the top layer and the substrate. In each of the three guides, there is a 0.4% index difference between the top and second layers, which gives single-mode propagation of the TE_0 and TM_0 mode in a 2 μm thick guide. Also, these structures have very little strain because of a less than 1% lattice mismatch between any of the layers and the GaAs substrate.

The mixed crystal layers are all basically ZnSe with small percentages of tellurium, cadmium, or sulfur. Films of $\text{ZnSe}_{0.98}\text{Te}_{0.02}$ have already been obtained, and we will obtain at least one of the three structures shown in figure 7 to test in the next few months.

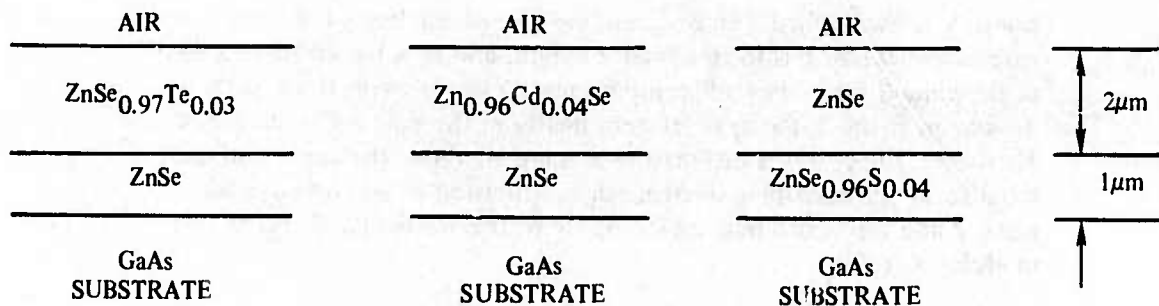


Figure 7. Three double-layer heteroepitaxial structures.

ELECTROOPTIC PHASE MODULATORS

The heteroepitaxial films and the diffused waveguides have large electrooptic coefficients (comparable to GaAs), high resistivities (10^4 to 10^{12} ohm-cm), and optical transmission in the visible and near infrared, making them desirable candidates for electrooptic modulation. All the structures except the $\text{CdS}_{1-x}\text{Se}_x$ diffused guides have an r_{41} electrooptic coefficient, which is characteristic of cubic zinc blende semiconductors such as GaAs. $\text{CdS}_{1-x}\text{Se}_x$ has the r_{13} , r_{33} , and r_{51} electrooptic coefficients characteristic of semiconductors with a uniaxial wurtzite structure (ref. 5).

The $n^3 r_{41}$ coefficients for some of these materials were given in table 3. Electric fields applied to them induce changes in the refractive index of several parts in 10^4 for fields around 10^5 V/cm , which is the order of the breakdown field in these materials. For example, 20 volts applied across a $2\mu\text{m}$ thick layer would produce this field.

Electrooptic phase modulators have been fabricated using the heteroepitaxial films as well as the diffused layer structures. The best results have been obtained in heteroepitaxial ZnSe on GaAs. One of the ZnSe modulators is shown in figure 8. An insulating layer of evaporated silicon monoxide partially oxidized to give SiO_x , with $1 < x < 2$, is placed on top of the guide to minimize losses of the guided wave in the aluminum electrode. The resistivity of the ZnSe layer is much higher than that of the GaAs substrate, so almost the entire voltage drop applied between the aluminum electrode and the InHg ohmic contact is across the ZnSe layer.

Light propagating along the ZnSe layer with an arbitrary polarization is composed of leaky modes that can be divided up into TE modes polarized in the (100) film plane and TM modes polarized normal to the film plane (ref. 4). A voltage drop across the ZnSe layer induces an electrooptic phase shift between each TE mode of a given order and its corresponding TM mode of the same order. For the i th TE and TM mode:

$$\phi_i(v) = \frac{\pi L}{\lambda} n_i^3 r_{41} \frac{V}{t}$$

where V is the applied voltage across the film of thickness t , λ is the free space wavelength, L is the modulator length, and n_i is the effective index of the guided wave. For a film more than 20 wavelengths thick, such as the one in figure 8, the n_i are all very nearly n , the bulk refractive index. Therefore, the ϕ_i of the different modes are all about the same; and the usual formulas describing electrooptic modulation between two orthogonal plane waves in a bulk crystal apply to this particular thin-film modulator (ref. 6):

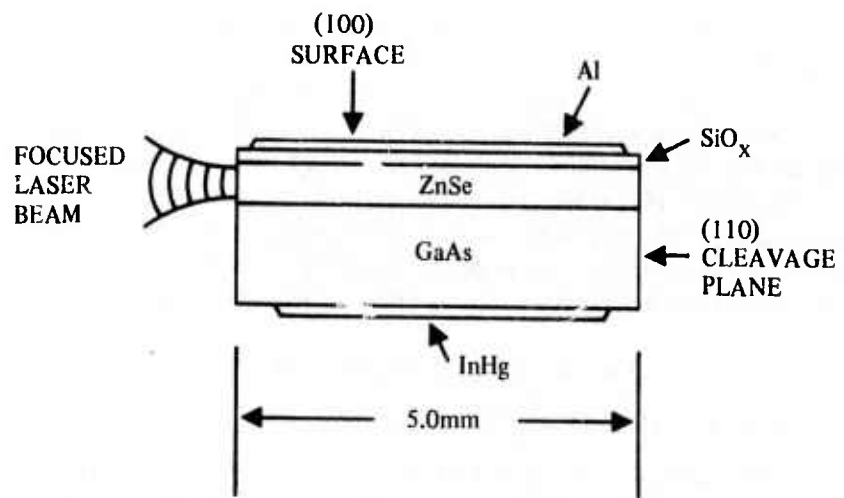
$$\phi(v) = \frac{\pi L}{\lambda} n^3 r_{41} \frac{V}{t}$$

The electrooptic phase shift between the two orthogonal components of the electric field yields the intensity-modulated output

$$I = I_0 \sin^2 \frac{\phi(V) + \phi_0}{2}$$

when light exiting the guide is passed through an analyzer aligned at 45° (ref. 6).

The setup to obtain the intensity modulation is shown in figure 9. The optical compensator is adjusted to give maximum modulation for a given applied voltage from the pulse generator, and the modulated output from the photomultiplier is observed as a trace on an oscilloscope.



LAYER THICKNESS RESISTIVITY INDEX

SiO _x	1200Å	10^7 ohm-cm	1.6
ZnSe	15μm	10^7 ohm-cm	2.58
GaAs	0.5mm	10^{-2} ohm-cm	3.9 - 0.1j

Figure 8. ZnSe heteroepitaxial thin-film phase modulator.

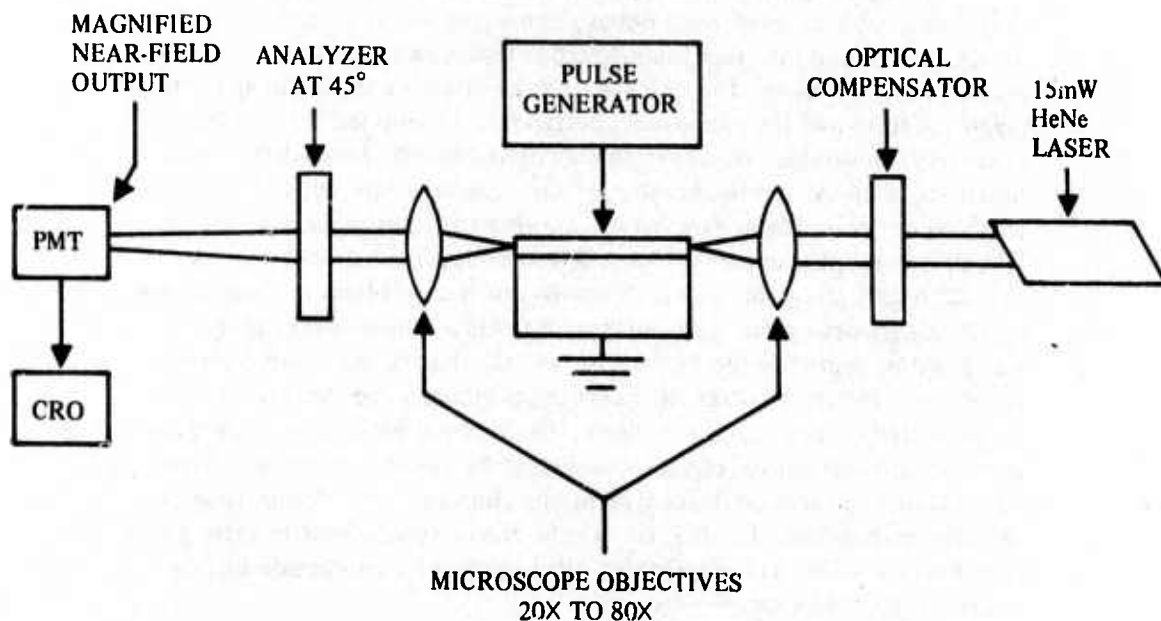


Figure 9. Intensity modulator setup.

Modulation depths up to 60% have been observed between a voltage "on" state at 100 volts and an "off" state at 0 volts, with a switching time from the "off" to "on" state of less than half a microsecond.

The ZnSe heteroepitaxial modulator, although crude, demonstrates the feasibility of electrooptic modulation in II-VI-compound heteroepitaxial structures. The moderately rapid switching speed is an encouraging development. With improved design, thin-film electrooptic modulators with very small electrodes and response times of a few nanoseconds should be obtained in the heteroepitaxial and diffused waveguide structures.

FIBER-OPTICAL WAVEGUIDES

GUIDED WAVES IN INHOMOGENEOUS FIBERS

Growing interest in the use of glass fibers as optical communication lines has provided the impetus in understanding the propagation characteristics of guided light along glass fibers. The problem of wave guiding along a circular homogeneous fiber was solved many years ago (ref. 7). Interesting results concerning the dispersive characteristics of various modes on this homogeneous fiber have been well tabulated. On the other hand, the problem of wave propagation along a radially inhomogeneous fiber has not been satisfactorily resolved. The inhomogeneity of the media may be caused by the unintentional diffusion effect or by intentional tailoring of the radial index of the refraction profile of a cylindrical fiber such as the Selfoc fiber. Unlike the homogeneous fiber case, the wave equation governing the fields for radially inhomogeneous fibers consists of two coupled second-order differential equations whose solutions are usually very difficult to obtain.

A useful approximate approach to an analytical solution of electromagnetic problems involving a radially inhomogeneous column is to subdivide the column into thin homogeneous layers and then solve an easier problem in each layer. The fields in each layer are expanded in appropriate eigenfunctions and the expansion coefficients determined by matching boundary conditions. However, this straightforward approach becomes much too tedious, and the number of simultaneous equations to be solved tends to be prohibitively large as the number of layers increases (ref. 8). It is therefore quite apparent that a different approach must be taken.

A general mathematical discussion of the problems of formulating equations governing the electromagnetic fields in inhomogeneous media was given by Nisbet in the 1950s (ref. 9). He showed that, under certain conditions, the electromagnetic fields in an inhomogeneous medium can be generated by two scalar functions. These conditions relate the order of the resultant differential equations satisfied by the electromagnetic field components to the coordinate system and the functional dependence of the inhomogeneities. Let (u_1, u_2, u_3) be the coordinates of an orthogonal curvilinear system. The elementary cell bounded by coordinate surfaces is a rectangular box whose edges are

$$ds_1 = h_1 du_1, \quad ds_2 = h_2 du_2, \quad ds_3 = h_3 du_3$$

and whose volume is

$$dv = h_1 h_2 h_3 du_1 du_2 du_3$$

Now, if two conditions are satisfied — h_3/h_2 is independent of u_1 , and ϵh_1 and h_1 are independent of u_2 and u_3 , where $\epsilon = \epsilon(u_1, u_2, u_3)$ — then it is possible to obtain second-order differential equations for the two scalar functions from which all electromagnetic field components may be derived. Otherwise, the differential equations may be of an order higher than the second. One notes that a spherically symmetric medium in which the dielectric variation is a function of the radius satisfies the two conditions, whereas a cylindrically symmetric medium with dielectric variation being a function of the radius does not. We may conclude that the present problem of the radially inhomogeneous cylinder is more complicated than that of the radially inhomogeneous sphere.

The purpose of the present investigation is to seek a way to solve the problem of guided waves in inhomogeneous fibers without the aforementioned difficulties and limitations. Recently, we developed a method that deals directly with the coupled differential equations and the appropriate boundary conditions (ref. 10). This method eliminates the need to evaluate untabulated functions or to invert large matrices.

Without loss of generality, one may assume that the expressions for the field components of all modes are multiplied by the factor $e^{in\theta + \beta z - i\omega t}$, which will be suppressed throughout. Maxwell's equations in matrix form then become

$$\frac{d}{dp} \vec{x} = \tilde{A} \vec{x} \quad (1)$$

where

$$\vec{x} = \begin{bmatrix} E_{zn} \\ \mu E_{\theta n} \\ \sqrt{\frac{\mu_0}{\epsilon_0}} H_{zn} \\ \rho \sqrt{\frac{\mu_0}{\epsilon_0}} H_{\theta n} \end{bmatrix}$$

$$\tilde{A} = \begin{bmatrix} 0 & 0 & -\frac{n\Gamma}{i\rho\epsilon/\epsilon_0} & \frac{1}{i\rho} \left(1 - \frac{\Gamma}{\epsilon/\epsilon_0}\right) \\ 0 & 0 & i \left(\rho - \frac{n^2}{\rho\epsilon/\epsilon_0}\right) & \frac{in\Gamma}{\rho\epsilon/\epsilon_0} \\ \frac{in\Gamma}{\rho} & \frac{i}{\rho} \left(\frac{\epsilon}{\epsilon_0} - \Gamma^2\right) & 0 & 0 \\ i \left(\frac{n^2}{\rho} - \rho \frac{\epsilon}{\epsilon_0}\right) & \frac{n\Gamma}{i\rho} & 0 & 0 \end{bmatrix}$$

$$\rho = k_0 r$$

$$\Gamma = \frac{\beta}{k_0}$$

$$k_0 = \omega \sqrt{\mu_0 \epsilon_0}$$

A fundamental matrix is found by integration from the relation

$$\tilde{x}(\rho_\alpha) = \beta(\rho_\alpha, \rho_0) \tilde{x}(\rho_0) \quad (2)$$

where $x(\rho_0)$ and $x(\rho_\alpha)$ are given by the relation

$$x(\rho_0) = [C, D] = \begin{bmatrix} Cc_1 \\ Cc_2 + Dd_2 \\ Dd_1 \\ Cc_3 + Dd_3 \end{bmatrix} \quad (3)$$

and

$$x(\rho_\alpha) = [E, F] = \begin{bmatrix} Ee_1 \\ Ee_2 + Ff_2 \\ Ff_1 \\ Ee_3 + Ff_3 \end{bmatrix} \quad (4)$$

C, D, E, and F are arbitrary constants, $\rho_0 = k_0 r_0$, and $\rho_\alpha = k_0 a$. Substituting equations (3) and (4) into equation (2) gives

$$\begin{bmatrix} e_1 & 0 & -(c_1 b_{11} + c_2 b_{12} + c_3 b_{14}) & -(d_2 b_{12} + d_1 b_{13} + d_3 b_{14}) \\ e_2 & f_2 & -(c_1 b_{21} + c_2 b_{22} + c_3 b_{24}) & -(d_2 b_{22} + d_1 b_{23} + d_3 b_{24}) \\ 0 & f_1 & -(c_1 b_{31} + c_2 b_{32} + c_3 b_{34}) & -(d_2 b_{32} + d_1 b_{33} + d_3 b_{34}) \\ e_3 & f_3 & -(c_1 b_{41} + c_2 b_{42} + c_3 b_{44}) & -(d_2 b_{42} + d_1 b_{43} + d_3 b_{44}) \end{bmatrix} \begin{bmatrix} E \\ F \\ C \\ D \end{bmatrix} = 0 \quad (5)$$

$c_{1,2,3}, d_{1,2,3}, e_{1,2,3}, f_{1,2,3}, b_{ij}$ ($i = 1..4, j = 1..4$) are all known functions. Setting the determinant of equation (5) to zero gives the dispersion relation of the guided wave problem. It is noted that the dielectric variation $\epsilon(\rho)/\epsilon_0$ may be a quite arbitrary function of ρ .

Computer programs for the above problem have been written. We are in the process of debugging the programs. Results of this investigation on the propagation of light along an inhomogeneous fiber will be published.

DISPERSION OF PULSES PASSING THROUGH FIBERS OR IOCs

It is well known that the information carrying capacity of a transmission line depends greatly on its dispersive characteristics. Distortion of the original pulse signal results when a pulse passes through a dispersive guiding structure. The dispersive characteristics of a light guide may be attributed to several major sources: the dispersion of various propagating modes, material dispersion, surface roughness, presence of scattering centers, bending of the guiding structure, deformation of the guide, and inhomogeneities of the guiding medium.

Let us assume that the frequency spectrum of an original input pulse signal, $s^i(t)$, is

$$s^i(\omega) = \int_{-\infty}^{\infty} s^i(t) e^{i\omega t} dt \quad (6)$$

Representing the dispersion characteristics of the fiber by a transfer function $T(\omega)$, one may easily show that the output frequency is given by

$$s^o(\omega) = T(\omega) s^i(\omega) \quad (7)$$

Hence, taking the inverse Fourier transform of the output signal, one obtains

$$s^o(t) = \frac{1}{2\pi} \int_{-\infty}^{\infty} T(\omega) s^i(\omega) e^{-i\omega t} d\omega \quad (8)$$

We are developing a computer program to perform the above operations; that is, knowing the input pulse signal $s^i(t)$ and the transfer function of the fiber, the program will be able to compute the expected output signal $s^o(t)$. The fast Fourier transform technique is being used.

By appropriately choosing the various mechanisms contributing to the degradation of the pulse (that is, $T(\omega)$) and by comparing the computed theoretical results from the above utility program with those obtained by measurement, we hope to isolate the major pulse deforming mechanisms for a given fiber guide.

NONCIRCULAR OPTICAL GUIDE

Complete solutions have been obtained only for the problems of wave propagation along a circular fiber or along plane thin-film waveguides. In practice, optical waveguides may take many different shapes. For example, the most natural shape of an integrated optical guide is that of a thin strip of dielectric constant ϵ_1 and width "a" supported by a substrate of dielectric constant ϵ_2 . Optical fiber guides may also possess cross-sectional shapes that are not circular. The need to solve for the propagation characteristics of waves on these guides is quite obvious. However, extreme analytical difficulties are encountered when fiber guides with noncircular cross sections are considered. Fortunately, a deformed circular fiber can usually be approximated by an elliptical fiber. Depending upon the eccentricity of the elliptical fiber, it can take the form of a circular fiber or of a flat tape fiber. An exact solution, although very involved, does exist for the elliptical dielectric waveguide problem. Results are expressed in terms of Mathieu functions. The problem of the dominant mode propagation along an elliptical fiber guide has been treated some time ago. The present investigation will deal with the propagation characteristics of high-order modes. Expressing the fields in terms of Mathieu functions and matching the appropriate boundary conditions, one obtains the set of equations for all modes:

$$A_n a_n = \sum_{r=0}^{\infty} L_r \ell_r \alpha_{r,n}$$

$$B_n b_n = \sum_{r=1}^{\infty} P_r \rho_r \beta_{r,n}$$

$$\frac{\omega \epsilon_1}{\beta} B_n b_n' + \left(1 + \frac{\gamma_1^2}{\gamma_0^2}\right) \sum_{r=0}^{\infty} A_r a_r x_{r,n} = - \left(\frac{\gamma_1^2}{\gamma_0^2}\right) \frac{\omega \epsilon_0}{\beta} \sum_{r=1}^{\infty} P_r \rho_r' \beta_{r,n}$$

$$\frac{\omega \mu}{\beta} A_n a_n' - \left(1 + \frac{\gamma_1^2}{\gamma_0^2}\right) \sum_{r=0}^{\infty} B_r b_r \nu_{r,n} = - \left(\frac{\gamma_1^2}{\gamma_0^2}\right) \frac{\omega \mu}{\beta} \sum_{r=1}^{\infty} L_r \ell_r' \alpha_{r,n}$$

($n = 0, 2, 4 \dots$, or $n = 1, 3, 5 \dots$)

where

$$\gamma_1^2 = \frac{1}{4} (k_1^2 - \beta^2) f^2, \gamma_0^2 = \frac{1}{4} (\beta^2 - k_0^2) f^2, k_{1,0}^2 = \omega^2 \mu \epsilon_{1,0},$$

f is the semi-focal length, and β is the propagation constant, and ϵ_1 and ϵ_0 are, respectively, the dielectric constant of the fiber and that of its cladding. A_r, B_r, P_r , and L_r are arbitrary constants. $a_n, b_n, p_n, \ell_n, \alpha_{r,n}, \beta_{r,n}, x_{r,n}$, and $\nu_{r,n}$ are known constants expressible in terms of Mathieu functions. Setting the infinite determinant of the set of linear algebraic equations to zero gives the dispersion relation of various modes on an elliptical dielectric fiber.

We have initiated the task of writing a computer program to solve this infinite determinant for the propagation constants of various modes. It is believed that this program will be ready for debugging within the next three months. The complexity of this problem will not be underestimated.

SUMMARY AND PROJECTION

The concept of miniature optical components interconnected via optical waveguides on transparent dielectric substrates is attractive from the standpoints of military information transfer and high-capacity (multi-GHz) telecommunications. Optical sources, modulators, detectors, filters, couplers, etc., might be incorporated into "circuits" — analogous to integrated electronic circuits — which would execute a variety of functions with significant cost-performance advantages.

A great stimulus to integrated optics has been the advent of low-loss (<20dB/km), single-mode (>10Gbits/sec over a km length) glass-fiber waveguides; integrated optics would provide the necessary modulation bandwidth (at higher efficiency) required to match these waveguides. A major interest in integrated optics from a military system standpoint is the potential for implementing a fiber-optic-transmission-line, multiterminal multiplexing system through low-loss integrated optic coupling and modulation elements. This would offer isolated-terminal, EMI-free, redundant, fail-operative information transfer, thus facilitating the truly modular (including distributed computer) command control and communication system.

The objective of the program reported here is to advance the material and device physics of integrated optics for military applications, to establish in concert with other Navy and DoD programs a continuing assessment of system requirements, and to produce prototype optical elements and subsystems which are aimed at satisfying these requirements.

The task of circuit conception and design will be a continuing one, stemming from the technology and application assessment. Through the program, elementary circuits and subsystems will be fabricated, and an experimental IOC fiber-optic communication system will be investigated.

Research and development is being performed in the following areas:

1. Optical waveguiding in diffused-layer and heteroepitaxial thin film semiconductor structures, both planar and three dimensional
2. Electrooptic modulation in diffused-layer and heteroepitaxial thin-film semiconductor structures of high resistivity
3. Pattern delineation of miniature three-dimensional waveguides and related optical elements by photo- and electron-resist masking techniques and by ion beam milling
4. Optical coupling of light into and out of integrated optic circuits, in particular using fiber-optic waveguides
5. Theoretical analysis of optical propagation in a variety of waveguide structures to support work in the preceding research areas

The body of this technical report discussed the work already accomplished in tasks 1 and 2 at NELC up to October 1972. The work in tasks 3, 4, and 5 is just beginning, with the bulk of it to be performed at the Hughes Research Laboratories (task 3), the University of Washington (task 4), and the University of California, Los Angeles (task 5).

The work already performed in task 5 was covered in the FIBER-OPTICAL WAVEGUIDES section of this report. Three theoretical topics on the propagation characteristics of light in fiber-optic waveguides are currently being pursued. They are:

1. Guided waves in circular fibers, with an arbitrary radial index profile
2. Spreading of light pulses passing through fibers or films from material dispersion, scattering centers, etc.
3. Guided waves in fibers and other guides of noncircular symmetry, in particular in fibers of elliptical symmetry where exact although complicated solutions have been worked out

Technical results obtained so far at NELC are:

1. The fabrication of planar optical waveguides by diffusion in II-VI compounds
2. The observation and analysis of waveguiding in II-VI, III-V heteroepitaxial structures.
3. The fabrication of tiny three-dimensional waveguides by diffusion in II-VI compounds using shadow masking techniques
4. The fabrication of electrooptic-waveguide phase modulators in diffused II-VI structures and in II-VI, III-V heteroepitaxial structures

The feasibility of low-loss optical waveguiding (1dB/cm) and rapid electro-optic modulation (up to 1GHz) is being explored in these structures. The diffused single-crystal waveguides are made by diffusing cadmium or selenium into ZnSe, CdS, and ZnS crystals using the simple closed-tube method

described above under DIFFUSED WAVEGUIDES (see table 1 and figure 2). Changes in refractive index up to 5% are easily obtained this way by controlling diffusion times, temperatures, and initial conditions. Planar and three-dimensional guides with cross-sectional areas as small as 2 by 5 μ m and losses less than 3dB/cm have been achieved in cadmium-diffused ZnSe (see figures 4 and 5).

Heteroepitaxial films of ZnSe and ZnS on GaAs are also being considered. ZnSe on GaAs, in particular, shows promise because of the very close lattice match between the GaAs substrate and the ZnSe film (see table 3) and because of the very high resistivity (up to 10^{10} ohm-cm) of the ZnSe film, which is desirable for electrooptic modulation. Phase modulators have been constructed to demonstrate the feasibility of guided-wave electrooptic modulation in these films (see figures 8 and 9). The response times of a few hundred nanoseconds in these prototype modulators should be lowered by two orders of magnitude with improved design and electrode miniaturization.

More complicated waveguide patterns will soon be investigated in the diffused and heteroepitaxial structures. A clean room has been set up with facilities for photo-resist masking (spinner, mask aligner, etc.) and a Brandex sputtering system to sputter deposit films of SiO₂ onto the semiconductor substrates and to sputter etch patterns into the substrates. Electrooptic phase modulators consisting of miniature electrodes on top of channel waveguides will be constructed first, to be followed by more complicated structures such as directional couplers, both passive and electro-optically active, and electrooptic grating deflectors.

In conclusion, a variety of waveguides and waveguide modulators will be fabricated and evaluated in the next year in the diffused and heteroepitaxial structures.

REFERENCES

1. Taylor, H. F., Martin, W. E., Hall, D. B., and Smiley, V. N., "Fabrication of Single Crystal Semiconductor Optical Waveguides by Solid State Diffusion," Applied Physics Letters, v. 21, p. 95, August 1972
2. Martin, W. E., and Hall, D. B., "Optical Waveguides by Diffusion in II-VI Compounds," Applied Physics Letters, v. 21, p. 325, October 1972
3. Hall, D. B., and Martin, W. E., Proceedings of the VII International Quantum Electronics Conference, Montreal, Canada, May 1972
4. Hall, D. B., and Yeh, C., "Leaky Waves in a Heteroepitaxial Film," Journal of Applied Physics, to be published
5. Kaminow, I. P., and Turner, E. H., "Linear Electrooptic Materials," Handbook of Lasers, ed. R. J. Pressley, CRC Press, 1971
6. Yariv, A., Quantum Electronics, Wiley & Sons, 1967
7. Snitzer, E., "Cylindrical Dielectric Waveguide Modes," Journal of the Optical Society of America, v. 51, p. 491, May 1961
8. Wait, J. R., "Some Boundary Value Problems Involving Plasma Media," Journal of Research of the National Bureau of Standards - B. Mathematics and Mathematical Physics, v. 65B, p. 137, 1971
9. Nisbet, A., "Electromagnetic Potentials in a Heterogeneous Non-conducting Medium," Proceedings of the Royal Society of London - A. Mathematical and Physical Sciences, v. 240, p. 375, 1957
10. Yeh, C., and Wang, P. K. C., "Scattering of Obliquely Incident Waves by Inhomogeneous Fibers," Journal of Applied Physics, v. 43, p. 3999, October 1972